Low loss, high contrast optical waveguides based on CMOS compatible LPCVD processing

R.G.Heideman (1), D. Geuzebroek (1), A. Leinse (1), A. Melloni (2), F. Morichetti (2), C. Roeloffzen (3), A. Meijerink (3), L. Zhuang (3), W. van Etten (3), E. Klein (4) and A. Driessen (4).

1) LioniX bv, P.O. Box 456, 7500 AH Enschede, the Netherlands
2) Dipartimento di Electronica e Informazione, Politechnico di Milano, Via Ponzio 34/5, 20133 Milano, Italy
3) Telecommunication Engineering group, Faculty of Electrical Engineering, MCS, University of Twente, P.O.Box 217, 7500 AE, Enschede, the Netherlands
4) Integrated Optical Micro Systems, MESA$^+$ Research Institute, University of Twente, P.O. Box 217, 7500 AE Enschede, The Netherlands

Abstract: *A new class of integrated optical waveguide structures is presented, based on low cost CMOS compatible LPCVD processing. This technology allows for medium and high index contrast waveguides with very low channel attenuation. The geometry is basically formed by a rectangular cross-section silicon nitride (Si_3N_4) filled with and encapsulated by silicon dioxide (SiO_2). The birefringence and minimal bend radius of the waveguide is completely controlled by the geometry of the waveguide layer structures. Experiments on typical geometries will be presented, showing excellent characteristics (channel attenuation ≤ 0.06 dB/cm, IL ≤ 0.6 dB, PDL ≤ 0.2 dB, Bg «1×10^{-3}, bend radius ≤ 500 μm).*

Introduction

As demand for telecommunication bandwidth increases and the optical fiber networks move steadily towards the customer premises, demand for optical switching and routing components is rising. As a consequence, optical components are replacing electronics for signal processing [1-3]. The adoption rate for optical components is being hampered, however, by their high costs stemming from two major sources: large optical footprint (i.e. high chip real-estate) and high packaging costs. By integrating multiple functions at a higher density on a single optical chip much of these costs can be amortized across several devices. In order to achieve a high density photonic platform, the index contrast and channel attenuation of the waveguide must be sufficiently large and small enough, respectively, to allow for tight curvature and cascading of multiple structures. This opens the pathway to use micro ring resonators as the universal building block in systems capable of providing switching and routing functionality [1,2,4-6].

A new waveguiding technology, designed, developed and patented by by LioniX BV is capable of meeting these demands outlined above. It comprises of alternating CMOS-compatible LPCVD layers which are fully transparent for wavelengths from < 500 nm up to 2 μm and beyond. The technology allows for medium and high index contrast waveguides. In this paper we describe the fabrication and performance of three typical waveguide geometries and give examples of (realized) applications. Both designs exhibit very low waveguide attenuation values but otherwise have totally different characteristics and applications..

Waveguide concept

Stoichiometric silicon nitride (Si_3N_4) fabricated using LPCVD processing is widely used in integrated optics, primarily because of its large refractive index (2.0) enabling very compact devices [2,6,10]. The major drawback of Si_3N_4 is its large internal tensile stress (~1GPa) which limits its layer thickness to ≤350 nm. As a consequence devices fabricated with

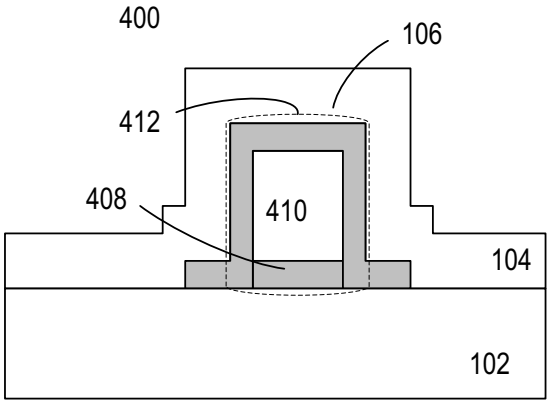

Fig. 1: Cross-section of a typical waveguide structure, with LPCVD Si_3N_4 (in grey) as basic waveguiding layer, filled with and in turn encapsulated by SiO_2 (white). Figure extracted from [7]

Si_3N_4 show a very large polarization dependency, thereby severely limiting their use in telecom applications. By combining it with a second layer that has a very large compressive stress, such as LPCVD SiO_2 (TEOS), however, the total stress of the composite layer stack is strongly reduced. As a result the thickness of the total stack can be considerably larger than the critical layer thickness of Si_3N_4 alone [7,8].

This alternating LPCVD layer stack concept can result in a rectangular channel waveguide structure with outstanding waveguiding characteristics and with strongly reduced polarization effects. The geometry is basically formed by a rectangular cross-section of silicon nitride (Si_3N_4) filled with and en-

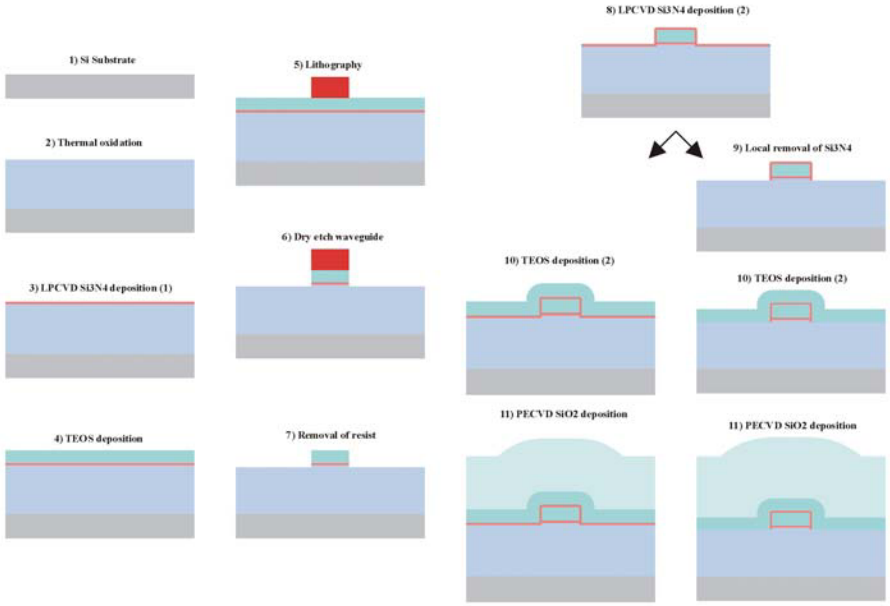

Fig. 2: Flow process scheme as made with Flowdesigner process modeler (PhoeniX BV, Enschede, the Netherlands). Here, the $Si_3N_4$is shown in red, and the (different types of) SiO_2 in blue. For explanation, see text.

capsulated by silicon dioxide (SiO_2) as depicted in figure 1.

The channel geometry approximates a "hollow core" system, as it consists of a low index "inner core" of SiO_2 "cladded" with the high index "outer core" of Si_3N_4. The channel is fabricated on a substrate, e.g. thermally oxidized silicon. The nitride shell has typical outer dimensions in the order of 1 μm^2, with its exact characteristics depending strongly upon the desired application.

Modal characteristics depend only upon the geometry of the structure, as all composing materials are LPCVD end products with very reproducible characteristics. The whole process is CMOS-compatible and very cost effective as only one photo lithographical step is required. In this paper, we will describe three different waveguide geometries based upon this procedure, all going with excellent attenuation values but with strongly deviating modal characteristics. Some applications will be elucidated.

Fabrication

Figure 2 depicts the LioniX fabrication procedure for passive optical channels for two of the three different variations of the waveguide geometry. The fabrication process of all variations starts with thermal oxidation of a 100 mm-diameter silicon wafer (1 and 2) to form the lower cladding. Then LPCVD Si_3N_4 (3) and TEOS SiO_2 (4) are deposited. Photolithography is then performed (5), followed by RIE (6), and photo resist removal (7). After a second deposition of LPCVD Si_3N_4 (8), the top cladding can be deposited with or without local removal of the slab nitride layer (9). Without the local removal of this nitride layer, the fabrication process is simplified but also goes with remaining slab waveguiding effects. Local removal of nitride, although more difficult in fabrication, results in the box-shaped structure going with even further reduction of modal birefringence and, also important, absence of slab waveguides. The last two steps for both options are TEOS deposition and PECVD oxide deposition (10 and 11, respectively) to form the upper cladding. The third geometry -not depicted in figure 2- only deviates in the etching process: in this layout, the bottom nitride layer is only partly etched, see figure 3 (left): this results in a strongly asymmetric waveguide layout going with large modal birefringence.

Although of major importance, the design of the channel waveguides falls beyond the scope of these proceedings and will be described in other publications. Here, we restrict ourselves to three examples of single mode (SM @1550 nm) channel layouts, see figure 3:

1: a non-symmetrical layout with very large modal birefringence (see figure 3, left)

2: an A-shaped layout with strongly reduced modal birefringence (see figure 3, center)

3: a box-shaped layout, with minimal modal birefringence (see figure 3, right and also [9]).

Layout 1 demonstrates the ability to tune to large modal birefringence combined with tight bending radii, at relaxed fabrication tolerances. Here the RIE procedure (which, as explained, is performed before the TEOS deposition) removes approximately only half of the first nitride layer thickness. This layout is used in a tunable true time delay (TTD) application, as described later in this paper (see also [10]). Here the channel waveguide is activated by means of heaters fabricated on the top cladding, exploiting the well-known thermo-optical effect [6].

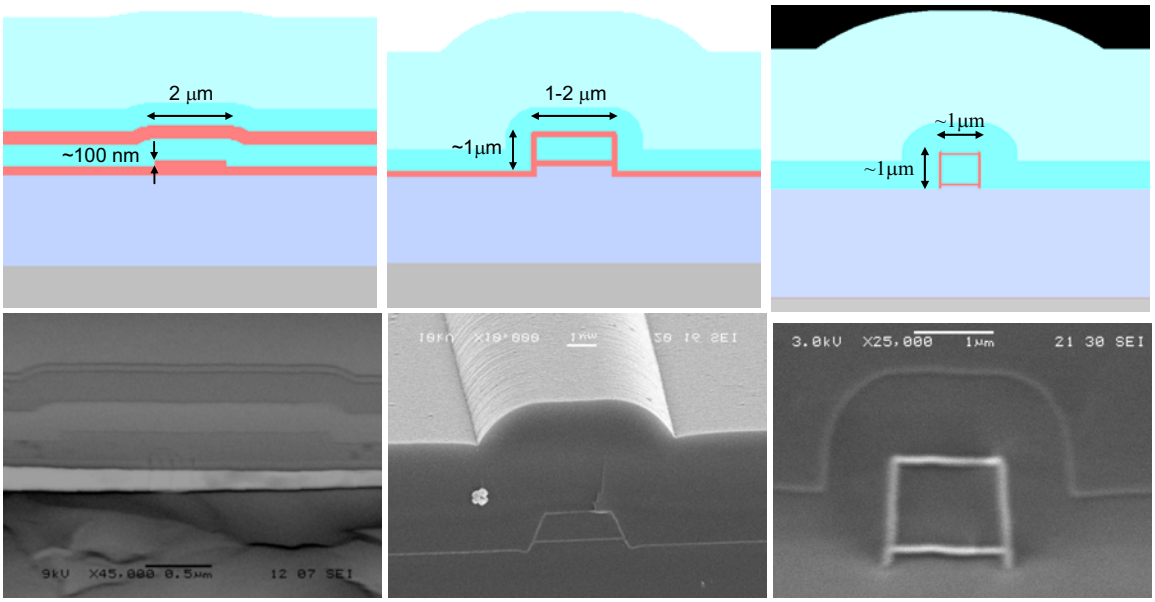

Fig. 3: Schematics (top) and corresponding SEM pictures of realized structures (bottom) of three typical channel layouts: a non-symmetrical layout with very large modal birefringence (left), an A-shaped layout with strongly reduced modal birefringence (center) and a box-shaped layout with minimal modal birefringence (right). The nitride layers are shown in red in the schematic view.

Layouts 2 and 3 show a much reduced polarization dependency, which can be understood in terms of symmetry in the geometry. In both cases, the anisotropic RIE etch step (see figure 2, step 6) completely removes the TEOS and Si_3N_4 layer as well as part of the thermal oxide layer. The following nitride deposition and subsequent top cladding layer deposition therefore results in a more rectangular layout. Both the A-shape (structure 2) as well as the box-shape (structure 3) can be tailored such, that almost no modal birefringence is resulting. Although easier to fabricate, the A-shape has the disadvantage of a remaining nitride slab layer. This is not the case for the third layout, the box-shape, in which the Si_3N_4 layer is locally removed: for telecom applications, this seems to be the most promising layout [9].

Results

The cross-section of the typical waveguides, as fabricated by LioniX, are shown in figure 3, bottom. Clearly visible is the close agreement with the designs of all structures.

The optical characterization is performed using different techniques, including cut-back and phase-sensitive optical low coherence interferometry [9]. These measurements are performed on a variety of differently processed wafers, showing a wide range of parameter settings. Key characteristics as measured on the best samples are given below in Table 1.

Several important conclusions can be drawn from these results. First the optical channel attenuation is very small for all types of geometries, while further improvement in performance is expected. Secondly, the IL is very small for both the A-shaped and (especially) the box-shaped geometries. Thirdly, for the A-shaped and boxed-shaped waveguides, the birefringence can be made very close to zero. Besides, all presented birefringence values are in good agreement with expectations, and therefore perfectly adjustable [9]. Fourth, the PDL is also small. The slightly larger PDL of the box-shaped can be completely attributed to a not-yet optimized fabrication procedure. Finally, all presented structures show reasonably small bending radii, also in line with theoretical predictions.

Two different applications with these waveguide geometries will be discussed hereafter.

Table 1: Measured characteristics on the best samples of the three types of SM channel waveguides.

	Non-symmetrical layout [1]	A-shaped geometry [1]	Box-shaped geometry [2]
Channel attenuation (dB/cm)	0.12	0.10	0.06
Insertion loss (IL) without spot size converter (dB) [3]	8.0	1.4	0.6
Group birefringence (B_g)	$\sim 1\times10^{-1}$	$\ll 1\times10^{-3}$	$\ll 1\times10^{-3}$
Polarization dependent loss (PDL, in dB) [3]	0.20	0.12	0.38
Minimal bend radius (µm)	400	750	500

[1]: chip length 3 cm
[2]: chip length 6¼ cm
[3]: here, small core fibers were used (MFD of 3.5 µm)

Application 1: Beamforming network

Beam forming for broadband RF signals can be achieved by means of a phased-array antenna working with an optical beam forming network (OBFN). This OBFN consists of optical splitting/combining circuitry and delay elements, which need to be continuously tunable in order to achieve continuous beam angle control. Moreover, in order to support relatively broadband RF signals, the delay elements should have a flat magnitude response and a linear phase response in the corresponding frequency range. To meet these requirements, optical ring resonators (ORR's) appear to be good candidates due to their continuous tunability, and well-known advantages of integrated optics [11-15]. Obviously, the waveguide technology used should provide small IL and especially small attenuation values, as substantial optical path lengths are required. Besides, a small bending radius is preferred, as this goes with small optical footprints (eg. reduced costs). In this section the advantages of optical beam forming using integrated ORR's are demonstrated, by explaining its operating principles, and by presenting some measurement results on an actual ORR-based 1x8 OBFN chip. As modal interference should be avoided, a polarization maintaining waveguide layout is preferred. Therefore, the chip is realized in layout 1 of the TriPleX-technology [16].

A single ring resonator shows a periodic bell-shaped group delay response. The peak delay value and its position are determined by the coupling coefficient and the additional round-trip phase shift of the ring, respectively. The bandwidth of the delay element can be increased by cascading multiple ORR sections. As the group delay responses of the individual sections simply add up, the total delay response can be flattened by properly tuning the ORR's [11, 13-15].

When the optical delay elements are integrated together with signal processing circuitry, an OBFN is obtained. In order to reduce the number of tuning elements, a binary tree OBFN topology is considered instead of the straightforward parallel OBFN. An ORR-based 1x8 OBFN has been proposed, consisting of 3 stages with in total 12 ORRs and 7 tunable splitters, as shown in Fig. 4.

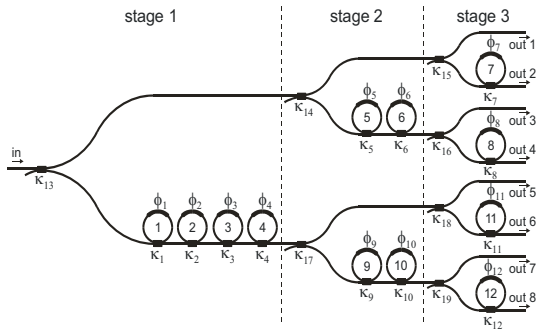

Fig. 4. Binary tree-based 1×8 optical beam forming network for a phased-array transmitter system, consisting of 12 ORR's and 7 tunable splitters.

Thr total size of the corresponding realized optical OBFN chip is only ~5 x 1 cm^2, see figure 5. This small footprint is clearly resulting from the reasonably small bending radius (see section "**Results**").

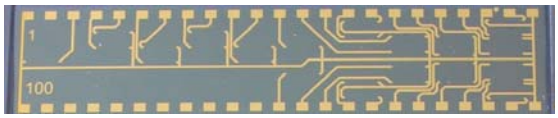

Fig. 5. Photograph of the realized 1x8 OBFN-chip, clearly showing the bondpads and heater electrodes. The chip size is ~5x1 cm^2.

Measurements have been carried out with different settings for the resistive heating elements, manufactured on top of these waveguides (sse section "**Fabrication**"). The measurement results verify the overall waveguide loss to be « 1 dB/cm.

Figure 6 shows the measured group delay responses at the outputs 2 to 8 of the OBFN, which demonstrate the delay generation of one single ring up to 7 cascaded rings. As a 1x8 OBFN, each output is required to give a different delay value over a common frequency band, in order to satisfy the condition of beam forming. Fig. 6 demonstrates linearly increasing delays from outputs 2 to 8 of the 1x8 OBFN chip, considering output 1 as the zero delay reference. The coupling coefficients and round-trip phase-shifts of the rings are tuned such that the delays cover a bandwidth of 2.5 GHz, with the largest delay value of approximately 1.2 ns (corresponding to 36 cm of physical distance in air) and delay ripple of approximately 0.1 ns (3 cm). Since the 1x8 OBFN chip is designed such that each of the 3 stages can be measured separately, in practice the final delay responses at the outputs are achieved by tuning every stage to a flattened delay response over a common frequency band before they add up.

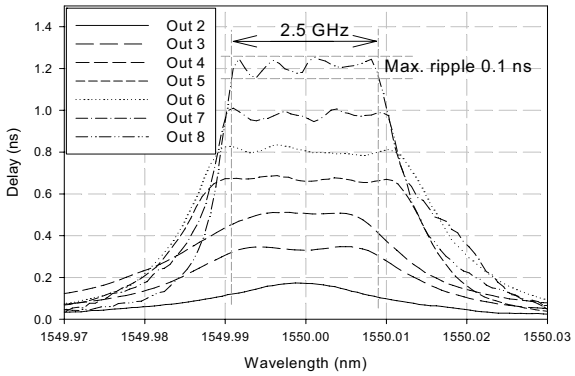

Fig. 6. Measured group delay responses at different outputs of the 1x8 OBFN chip.

Application 2: Microring resonators for telecom

The Microring Resonator (MR) represents a fundamental Planar Lightwave circuit (PLC) building block component. It is an integrated optics filter element with characteristics very similar to those of a

free-space Fabry-Perot filter.

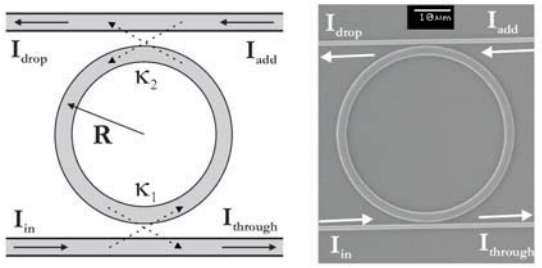

Fig 7. Schematics and picture of a single MR.

The MR offers the advantage, however, that injected and reflected signals are inherently separated into individual waveguides. In addition, since an MR does not require any facets or gratings, it is particularly simple to implement. MR's evolved from the fields of fiber optic ring resonators and micron scale droplets. Their inherently small size (with typical diameters in the range of several to tens of micrometers), filter characteristics, and potential for use in complex and flexible configurations, make these devices attractive for use in many integrated optics and VLSI photonics applications.
A basic schematic drawing of a MR is shown in Figure 7. The structure consists of a ring waveguide of radius R and two straight port waveguides.

The ability to tune a wavelength (MR resonance condition) is a highly desired aspect of the switching or routing function. Wavelength tuning enables better control of a specific wavelength by the network management system. There are several ways to make the MR tunable, but thermal tuning provides a low-cost solution.
Thermal tuning can be implemented by adding a small heater to the MR. When heated, the optical properties of an MR change and, as a result, the center wavelength of the switched wavelength signal is shifted. Thermal tuning is easy to implement with only the addition of a thin film heater on top of the MR.
The small area requirement of an MR enables integration of multiple devices in a limited space. Since they are all fabricated at one time, the cost of integrating tens to hundreds of individual MRs is low. As a result, highly complex system functionality can be provided within a small chip size at low overall cost.

An example of complex system functionality is a photonic switching and routing platform of which some examples are shown in figure 8. A photonic switching and routing platform can be produced by means of dense integration of MR filters. Such a platform enables development of flexible and reconfigurable network components such as optical switches, ROADMS, and dynamic gain equalizing filters.

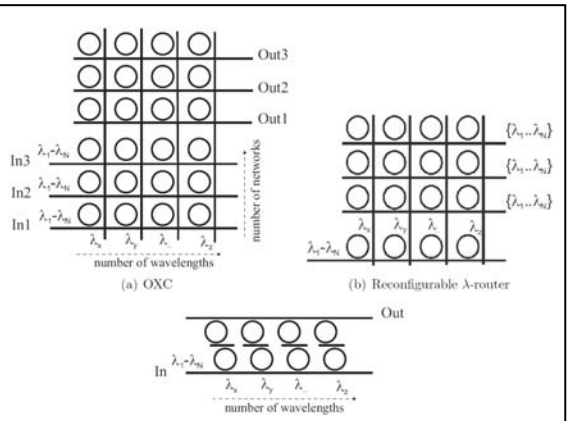

Fig. 8. Possible implementations of the photonic switching and routing platform.

The flexibility of the platform arises from the ability to combine multiple structures of different complexity on a single chip. In addition, individual tuning capability of each MR enables reconfigurability at the individual channel level.
Although MR's seem to be very versatile basic building block elements for VLSI photonic applications, their requirements on waveguiding technology are severe [1-4,18]. As mentioned, to obtain reasonable free spectal range (FSR) values, the MR should have a radius ≤ 50 μm, which can only be obtained using sufficiently high index waveguiding materials. A very suitable material is Si_3N_4, being one of the consisting components of the TriPleX technology. Based upon Si_3N_4, several nicely functioning demonstrators have been reported [18]. It is expected that these results can be improved when based upon TriPleX technology, due to the reported significantly smaller IL values. Currently, several fabrication batches are being processed, based upon MR designs exploiting the box-shaped layout previously described.

Conclusions

The TriPleX technology as been designed, patented and fabricated by LioniX is a CMOS compatible, LPCVD based technology showing very interesting features. Due to its very reproducible consisting materials, e.g. Si_3N_4 and SiO_2, the modal characteristics are determined only by the geometry of the waveguide. This enables a means to carefully control the modal birefringence from very small ($«1\times10^{-3}$) to extremely large values (for non-telecom applications wherein it is desirable to remove one polarization mode). The box-shaped and A-shaped layouts show nice modal overlaps with fiber modes, resulting in very small fiber-to-chip coupling losses (≤0.2 dB per facet). Combined with the small waveguide attenuation values (≤0.06 dB/cm), this results in very small IL values (≤0.6 dB), making the TriPleX technology very interesting for applications that require coupling into and out of the optical fiber network infrastructure. The reasonably small bending radii allow for small footprints, going with reduced cost price. For OBFN applications different demonstrators are fabri-

cated, showing very nice results. For routing and OADM applications, designs based on the box-shaped layout have been completed and batch fabrication is currently in progress. The reported results on the TriPleX technology demonstrate its high potentials for large-scale integrated optics.

Acknowledgments
This work is part of the Freeband BBPhotonics project (http://bbphotonics.freeband.nl). Freeband is sponsored by the Dutch government under contract BSIK 03025. This work is part of the Broadband Photonics beamformer project and the Smart project, Senter Novem project numbers ISO 52081 and ISO 53030, respectively. The Smart project is part of the European PIDEA$^+$ project SMART.

References

1 B.E.Little etal , IEEE Photon Technol. Lett., vol.12, pp.323-25, 2000.
2 A.Driessen et al, AIP conf. Proc., Vol. 709, pp.1-8, 2003.
3 C.K.Madsen, IEEE J. Ligthwave Technol., vol. 21, no.10, pp. 2412-20, 2003.
4 D. H. Geuzebroek et al, Wavelength filters for Fiber Optics, H. Venghaus (Ed.), 2006.
5 A.Melloni et al, Proc.Icton 2003(Warsaw), 2003.
6 D.H.Geuzebroek et al,Proc. ECIO 2003, pp. 395-398, 2003.
7 U.S. Patent application nr. 10/756627-001, “Low modal birefringent waveguides and methods of fabrication”, January 2004.
8 M.Melchiorri et al, Applied Phys. Lett., vol.86, pp. 121111-13 (2005).
9 A. Melloni et al, proceedings ECIO 2007, accepted for publication.
10 C.G.H.Roeloffzen, Proc. Leos Benelux Ch., pp 79-82, 2005.
11 G. Lenz, B. J. Eggleton, C. K. Madsen, R. E. Slusher, *IEEE J. Quantum Electron*., Vol. 37, No. 4, April 2001, pp. 525–532.
12 J. E. Heebner, V. Wong, A. Schweinsberg, R. W. Boyd, D. J. Jackson, *IEEE J. Quantum Electron.*, Vol. 40, No. 6, June 2004, pp. 726–730.
13 M. S. Rasras et al., *IEEE Photon. Technol. Lett.*, Vol. 17, No. 4, April 2005, pp. 834–836.
14 L. Zhuang, C. G. H. Roeloffzen, W. van Etten, *Proc. of the 12th IEEE/CVT Symp. in the Benelux*, Enschede, The Netherlands, Nov. 2005.
15 C. G. H. Roeloffzen, L. Zhuang, R. G. Heideman, A. Borreman, W. van Etten, *Proc. of the 9th IEEE/LEOS Symp. in the Benelux*, Mons, Belgium, December 2005, pp. 79–82.
16 R. G. Heideman, A. Melloni, M. Hoekman, A. Borreman, A. Leinse, F. Morichetti, *Proc. of the 9th IEEE/LEOS Symp. in the Benelux*, Mons, Belgium, December 2005, pp. 71–74.
17 L. Zhuang, C. G. H. Roeloffzen, R. G. Heideman, A. Borreman, A. Meijerink, W. van Etten, *Proc. of the International Topical Meeting on Microwave Photonics (MWP’2006)*, Grenoble, France, 3-6 October 2006, p. F1.4.
2005
18 E. Klein, Ph.D. thesis, April 2007.